Silicon micro-hemispheres with periodic nanoscale rings produced by the laser ablation of single crystalline silicon*

Chen Ming(陈 明)[a)†], Li Shuang(李 爽)[a)b)], Cui Qing-Qiang(崔清强)[a)], and Liu Xiang-Dong(刘向东)[a)c)‡]

[a)] School of Physics, Shandong University, Jinan 250100, China
[b)] School of Computer, Shandong Xiehe University, Jinan 250100, China
[c)] State Key Laboratory of Crystal Materials, Shandong University, Jinan 250100, China

(Received 4 March 2013; revised manuscript received 19 June 2013)

We describe the fabrication of silicon micro-hemispheres by adopting the conventional laser ablation of single crystalline silicon in the vacuum condition without using any catalysts or additives. The highly oriented structures of silicon micro-hemispheres exhibit many periodic nanoscale rings along their outer surfaces. We consider that the self-organized growth of silicon micro-structures is highly dependent on the laser intensity and background air medium. The difference between these surface modifications is attributed to the amount of laser energy deposited in the silicon material and the consequent cooling velocity.

Keywords: silicon micro-hemispheres, pulsed laser ablation

PACS: 61.46.Bc, 52.38.Mf **DOI:** 10.1088/1674-1056/22/10/106101

1. Introduction

With the development of photovoltaic solar and semiconductor industries, single-crystal silicon has been well known as excellent photo-detector and infrared window material.[1–4] In recent years, pulsed-laser-induced modification in the bulk of silicon materials has become a study topic of considerable interest, since the laser irradiation can lead to the dissociation of the compound semiconductor, increase the leakage current in photodiodes, etc.[1–7] On the other hand, laser ablation of silicon is important for the micro-fabrication of the thin films in semiconductor materials. Especially for high-density optical recording systems, laser-induced damage can give rise to the transformations from crystalline to amorphous state, which provides the difference in optical reflectivity between the crystalline and amorphous phase of the same single crystal silicon surface.[2–4,8]

Basic laser-induced modification involves the laser heating of substrate material, thermal stress, temperature gradient, grain re-crystallization, plasma expansion, etc., which are highly dependent on the laser parameters (such as intensity, wavelength, pulse width, number of shots), silicon surface morphology, background gas medium, etc. For many of the applications mentioned above, it is absolutely necessary to obtain full knowledge of the laser-induced modification in single-crystal silicon. By using short and ultra-short laser pulses (picosecond and femtosecond pulse width), many theoretical and experimental results have been obtained about the damage to silicon and silicon-based detectors.[2–4,7–9] It has been demonstrated that the interaction between a pulsed laser and single-crystal silicon is very complicated. The detailed mechanism involved in the laser-induced silicon micro-structures is still under debate and far from fully understood. In order to provide more information, we primarily focus on the self-organized growth of silicon micro-hemispherical structures by multiple pulses laser (1064 nm) ablation of single-crystal silicon. In the present study, the effects of laser intensity, cumulative pulses, and pressure of the background gas on silicon microstructure evolution are investigated by using scanning electron microscopy (SEM) and laser induced plasma emission spectroscopy (LIPES). The purpose of this work is to obtain an insight into the silicon surface modification by pulsed laser ablation operated at long wavelength. Meanwhile, the detailed discussion of these relevant physical processes is expected to inspire a deeper investigation for reshaping silicon surface morphologies by the laser thermal effect, which may exhibit particular applications for high-density optical recording systems.

2. Experiment setup

The experimental design used for pulsed-laser-induced modification and laser-induced plasma emission spectroscopy in Fig. 1 is similar to that adopted in our previous studies.[10–13] In brief, we chose crystal silicon with (100) orientation and double-sided polished as the target. The surface

*Project supported by the National Natural Science Foundation of China (Grant Nos. 11105085 and 11075097), the Excellent Youth and Middle Age Scientists Fund of Shandong Province, China (Grant No. BS2012CL024), and the Project of Higher Educational Science and Technology Program of Shandong Province, China (Grant No. J12LA51).

†Corresponding author. E-mail: chenming@sdu.edu.cn
‡Corresponding author. E-mail: xdliu@sdu.edu.cn

© 2013 Chinese Physical Society and IOP Publishing Ltd

modification of silicon was obtained at a relatively low gas pressure (3 Pa, defined as a "vacuum" condition in this paper) and in air (10^5 Pa), respectively. The pulsed-laser with a Gaussian profile from an Nd:YAG (yttrium aluminum garnet) laser (Quanta Ray, Spectra Physics) operated in fundamental IR (1064 nm) mode, with a pulse width of 10 ns and 5-Hz repetition rate. The laser beam was focused on the silicon target by a quartz lens (L1) with a 111-mm focal length. The power densities of the pulsed laser used in this experiment varied from ~ 7 GW/cm^2 to ~ 12 GW/cm^2, which was monitored by an energy meter (Molectron, EPM1000). Another 50-mm quartz lens (L2) was used to image the laser-induced plasma with a size of 1:1 onto the 10-μm-wide entrance slit of a spectrometer system. The spectrometer with 1200/mm grating (blazed at 300 nm) equipped with a time-gated (the used constant gate width of 5 ns) intensified CCD (ICCD) (DH740-18F-03, Andor Technology) was adopted to disperse the spectral emission from the plasma, and then collect the temporal spectral lines at different time delays with respect to the ablating laser pulse. The emission spectra were recorded at a distance of 2 mm from the target surface. After the pulsed laser ablation, the surface modifications and micro-structures were examined by using a field emission scanning electron microscope (Hitachi High-Tech) operated at 15 kV.

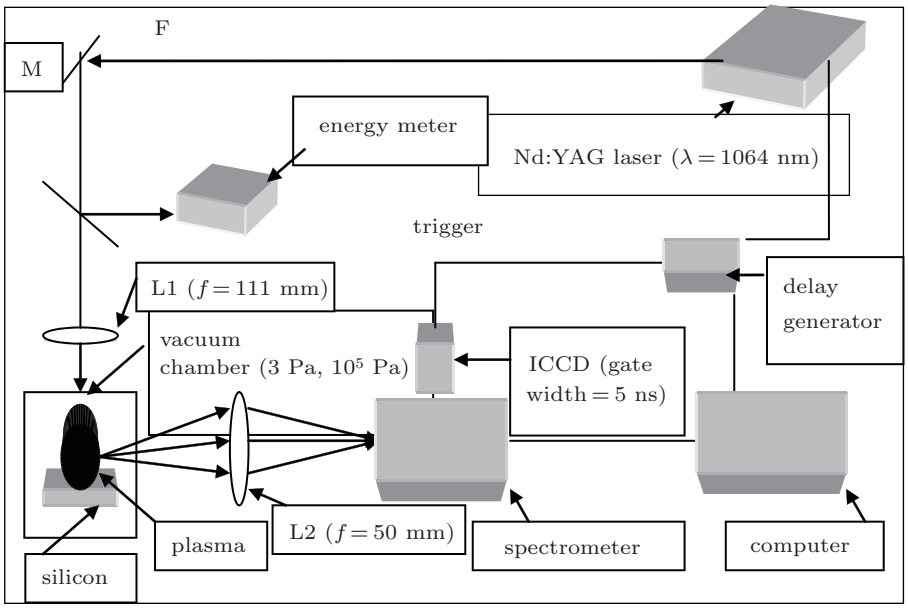


Fig. 1. Experimental set-up for laser-induced silicon modification and the laser-induced plasma emission spectrum.

3. Results and discussion

After five cumulative pulse ablations of the single-crystal silicon in vacuum conditions with a laser intensity of ~ 7.4 GW/cm^2, the typical surface modifications were examined by scanning electron microscopy, as shown in Fig. 2. The low-magnification image in Fig. 2(a) can be characterized by the circle-like crater with a relatively smooth bottom and the radiation pattern with numerous micro-grains flow from a central point to the periphery. As indicated in Fig. 2(b), the homogeneous distributions of these micro-grains are almost not hinge joints together, so they should be formed by nucleation process one by one separately. The pulse intensity ~ 7.4 GW/cm^2 used in this paper is high enough to ionize electron, converted into substrate heat energy, and then sharply increase the irradiating point temperature.[1] The irradiated silicon material is heated by a laser beam, followed by normal vaporization from the extreme outer surface. Meanwhile, the pulsed laser with a Gaussian profile preferentially leads to the formation of radial high temperature gradient imposed on the irradiated area. The radial powerful hydrodynamic pressure can make the melted silicon material flow from the core to the periphery, and break into micro-scaled grains. Finally, most of these heated silicon liquid grains are subjected to rapid cooling due to the expiration of the pulse and the exhaustive expansion of the vapor. On the other hand, we find that the faceted surfaces of the single pulse laser-produced silicon micro-structures are less clear than those obtained by multi-pulses, indicating that a feed-back mechanism is involved during the fabrication of highly oriented structures. As the next pulse laser arrives at the surface again, these previous surrounding debrises act as "seed" defects, which will result in a next preferential absorption laser energy. So a moderate number ($N = 5$) of laser pulses was adopted in this paper. If we further enlarge these individual grains, some more fasci-

nating regular micro-structures can be observed in Figs. 2(c) and 2(d). The magnified views reveal that the morphologies of silicon grains are characterized by highly center-symmetrical hemispheric structures with diameters of 2 μm ∼ 5 μm accreted on the tops of the stems. Moreover, the regular hemispherical silicon grain exhibits many screw-like periodic ring structures along its outer surface, which can be seen from the inset in Fig. 2(c). At the bottom region, the longitudinal distance between two rings is measured to be about ∼ 80 nm. While, the longitudinal gradient of these nanoscale ring structures gradually reduces from the hemispheric bottom to the top point. One point that should be emphasized is that the silicon micro-hemisphere with a concentric ring on its surface is quite similar to the ring structure obtained in a strong rotational flow polycarbonate melt,[14] and the system of concentric circles formed by a viscoelastic fluid in parallel-plate or cone/plate flows.[15] Based on previous discussions,[14,15] the existence of two phases with different rheological characteristics should result in the components consisting of different concentrations of solid particles. One component comes from a pure continuous phase with a first-order phase transition, and the other one includes filler chains.[14,15] In this paper, two phases with different hydromechanics characteristics in the early stage of the rapid cooling process can be expected to occur due to the inevitable high temperature gradient imposed on the molten silicon-grain. It seems reasonable to suppose that the phase separation and extension of liquid drops with the dispersed phase should play a critical role in forming the periodic ring structures on hemispheric silicon micro-grains. On the other hand, it is worth noting that the formation mechanism of these interesting silicon micro-structures is very complicated physical and chemical processes. In the following experiments, we show the evolution of silicon micro-structures as a function of the higher intensity pulse laser ablation and the pressure of the background air condition.

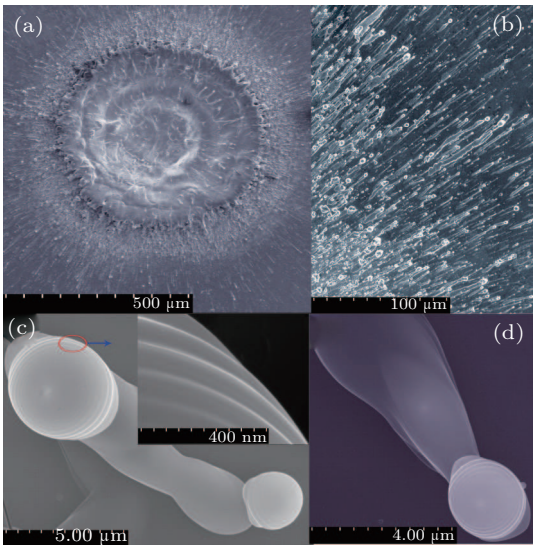


Fig. 2. (color online) (a) The overall morphologies of the irradiated single-crystal silicon surface formed by five pulses from a YAG laser operating at a wavelength of 1064 nm, pulse duration of 10 ns, and power density of 7.4 GW/cm^2 in vacuum condition (3 Pa). Panels (b)–(d) show closer views of the self-organized silicon hemispheric structures, revealing some regular screw-like periodic ring structures along its outer surface.

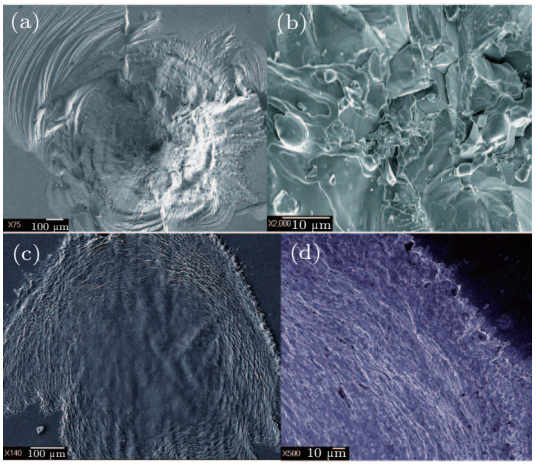


Fig. 3. (color online) (a) and (b) Typical SEM pictures (low and high magnification, respectively) taken from the ablated spot on a silicon target produced in vacuum conditions by five pulses with a laser incident intensity of 11.3 GW/cm^2. (c) and (d) SEM images (low and enlarged magnification, respectively) of the ablated silicon surface in air conditions by five pulses at an intensity of 7.4 GW/cm^2.

When the laser intensity increases from ∼ 7 GW/cm^2 to ∼ 12 GW/cm^2, the typical images of irradiated spot by the five-pulse laser ablation of silicon in vacuum conditions are displayed in Figs. 3(a) and 3(b). The overall morphology in Fig. 3(a) reveals that the higher laser intensity with 11.3 GW/cm^2 adopted in this paper preferentially leads to the formation of a deeper taper-like hole in the single-crystal silicon. The maximum surface diameter and depth of this cavity are measured to be about 2 mm and 500 μm, respectively, which are almost a factor of 2 larger and 50 deeper than those of the modified surface in Fig. 2(a). On the other hand, there are some irregular solidified drops formed on the bulk silicon fragments in the inner part around this conical structure, as shown in Fig. 3(b). Compared with the homogeneous silicon micro-grains observed in Fig. 2(b), the surface structure change in Fig. 3(b) involves a considerable decrease in the concentration of micro-grains at outside of the taper-like hole. As for the pulsed laser ablation in air conditions with an intensity of ∼ 7.4 GW/cm^2, the surface images are shown as in Figs. 3(c) and 3(d). The surface corrugations exhibit the formation of numerous ripple-like products with small waves flowing from the central point of the smooth molten area to the periphery. In contrast to the observation of a silicon micro-structure in vacuum conditions, we cannot see any individual regular silicon grains in Figs. 3(c) and 3(d). Meanwhile, other experiments (not shown here)

including the effects of laser wavelength (532 nm, 266 nm), laser shots (5 ∼ 200 pulses), etc. on the micro-structure evolution have been studied too.[16–20] Based on these experimental analyses, we confirm that the well-defined silicon microstructures are strongly dependent on laser intensity and background pressure, which are relatively insensitive to laser wavelength, multi-pulses, etc.

Laser-induced modification is highly related to the expanding plasma generated by laser ablation, therefore the early-stage evolution of plasma spectrum over a silicon surface were analyzed in this paper. As the laser intensity changes from 7.4 GW/cm^2 to 11.3 GW/cm^2, the temporal evolutions of spectral lines from Si ions (408.88 nm, 411.61 nm, 412.81 nm, and 413.09 nm) generated in vacuum conditions are displayed in Figs. 4(a) and 4(b), respectively. Then the peak intensities of the spectral line at 413.09 nm were measured for the delay time in a range of 65 ns∼1185 ns as shown in Fig. 4(c). According to the results in Figs. 4(a)–4(c), it is worth noting that the present time region of Si spectral lines ignited by a higher intensity laser is much earlier (time advance ∼ 170 ns) than that for the case of using lower-intensity laser. For example, the beginning of spectral lines at 413.09 nm can be fixed as early as at 65 ns, and the maximal peak intensity is located at a delay time of 385 ns with respect to the ablating laser pulse. While for lower-intensity laser radiation, these located times are drastically delayed at 235 ns and 560 ns, respectively. We also calculated the variation of plasma parameters (electron temperature and density) as a function of laser intensity. The electron temperature and density were calculated within a reasonable accuracy from the Boltzmann plot method and the Stark broadening of individual spectral lines, respectively, and the results are consistent with those in our previous work.[10–13] Since the curves of electron temperature and density versus delay time show a very similar tendency in this paper, the results of electron temperature regarded as a representative parameter are shown in Fig. 4(d). As for the higher intensity laser ablation, the peak electron temperature is about 4.42 eV at a delay time of 385 ns, which is nearly 2.6 times higher than that created by laser intensity ∼ 7.4 GW/cm^2. In the early stage of plasma evolution, we confirm that much hot and dense plasma by higher intensity laser irradiation expands faster than by a laser intensity of 7.4 GW/cm^2.

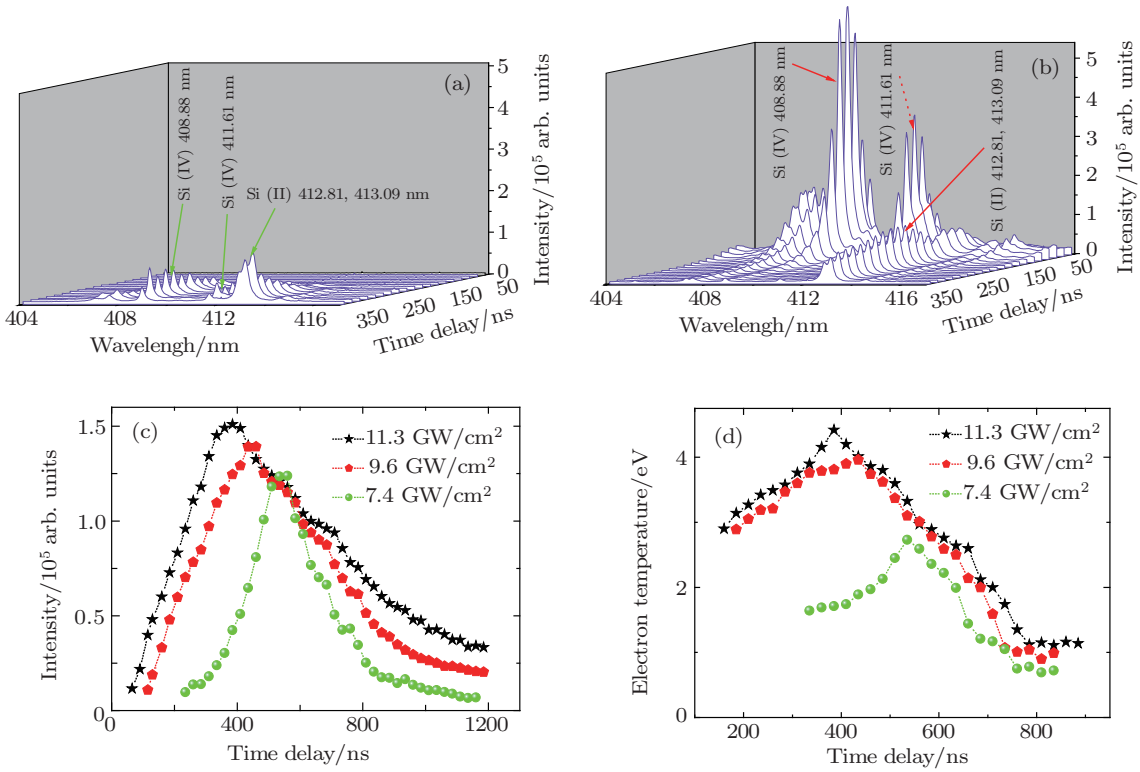


Fig. 4. (color online) (a) and (b) Early-stage evolutions of spectral lines emitted from Si atoms and ions in vacuum conditions, and the spectral lines generated by lasers with intensities of 7.4 GW/cm^2 and 11.3 GW/cm^2, respectively, which are measured at 2 mm from the silicon target surface. (c) The peak intensity of the emission spectral line from Si ions at 413.09 nm versus the delay time with respect to the ablating laser pulse. (d) The temporal evolution of electron temperature of the expanding plasma by three different laser intensities.

Therefore, we will provide a reasonable explanation for the regular silicon micro-structures evolution in this paper. As for the higher intensity laser used in this paper, surface superheating plays a critical role in the ablation process, and the phase explosion instead of normal boiling can cause numerous silicon materials to be directly converted from the solid stage to the gas stage. Moreover, structural modification by the first laser pulse can lead to an enhanced absorption of the following laser energy in the damage process by a subsequent laser beam. Therefore, the localized silicon material should be significantly removed from target, which is responsible for the observation of a taper-like hole in Fig. 3(a). As shown in Fig. 4, the hotter plasma will expand faster in the early stage of plasma evolution, which can offer additional energy to the ejected molten silicon material. The interaction of hotter plasma with molten silicon should significantly weaken the cooling process after laser irradiation. In this way, the dispersed phase in a shear stream followed by the regular phase separation in rapid cooling process will play a less important role in forming the reshaped silicon drop. As for the laser irradiation confined in atmospheric background conditions, the significant collision effect between the background gas and laser ignited plasma should be taken into account. The early evolutions of oxygen spectral lines at 777.19 nm, 777.42 nm, and 777.64 nm in vacuum and air conditions are displayed in Figs. 5(a) and 5(b), respectively. Compared with the oxygen spectral lines in vacuum conditions, high intensity continuum emission dominates the emission spectrum in the early stage (delay time within 600 ns) of the plasma evolution in the background gas. Based on the discussion in a previous study,[21] photo-ionization absorption takes a major role in initiating the air excitation and vaporization before a laser beam arrives at a target surface. Laser-induced air sparking and ionization are the main reason for the continuum emission observed in Fig. 5(b). Once the air vaporization is triggered near the silicon surface, the amount of laser energy can be considerably attenuated via the excited air plasma shielding and absorption before the laser beam reaches the silicon surface. The quantitative description[21] by Giacomo and Pascale[21] indeed suggested that about 76% of the original laser energy can be absorbed by air breakdown and consequent plasma. As expected in Fig. 3(c), the modified radiation areas are subjected really superficial damage in background medium, which is the consequence of the coupled effect of laser-induced air breakdown at the first step and then incident laser ablation of the silicon surface. On the other hand, the author's previous work[10] on laser-induced SiC plasma confirmed that the background pressure could increase the plasma lifetime substantially, which also holds true in this paper. When the silicon target is irradiated in background air, the laser-induced silicon plasma can create a higher shock wave with long-lived excitations. Due to the contribution of the trapped shock wave imposed on the molten silicon surface and the interaction of hotter plasma with the air medium, there is no appropriate condition for the rapid cooling process to occur in the early stage of laser ablation silicon. Consequently, we can see numerous ripple-like silicon structures instead of the well-defined micro-grains shown in Figs. 3(c) and 3(d). Overall, the analysis provides a reasonable qualitative description of the experimental results obtained in this paper.

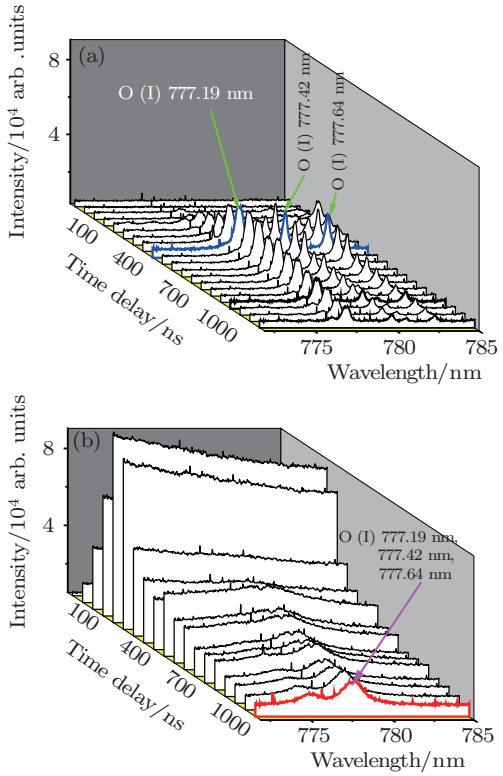


Fig. 5. (color online) Temporal evolution of the spectral lines generated from oxygen atoms in the expanding plasma at an incident laser intensity of 7.4 GW/cm^2 created in a vacuum condition (a) and in a background air medium (b).

4. Conclusions

In the present paper, the center-symmetric structures of silicon micro-hemispheres with concentric rings on the outer surface are generated by the pulsed-laser ablation of single crystal silicon in vacuum conditions with a pulse intensity of 7.4 GW/cm^2. It is found that these self-organized micro-grains can sharply decrease under relatively high laser irradiation, and completely disappear in air conditions. A qualitative discussion about the micro-structure change is proposed based on the dispersed phase within the early stage of the rapidly cooling process, laser-induced air breakdown, and the interaction between plasma and air.

References

[1] Wang X, Shen Z H, Lu J and Ni X W 2010 *J. Appl. Phys.* **108** 033103

[2] Umezu I and Sugimura A 2007 *Phys. Rev. B* **76** 045328
[3] Dachraoui H and Husinsky W 2006 *Phys. Rev. Lett.* **97** 107601
[4] Lorazo P, Lewis L J and Meunier M 2006 *Phys. Rev. B* **73** 134108
[5] Arora V K and Dawar A L 1996 *Appl. Opt.* **35** 7061
[6] Chen Y B, Lu J and Ni X W 2007 *Proc. SPIE* **6835** 68351X-1
[7] Cultrer L, Zeifman M I and Perrone A 2006 *Phys. Rev. B* **73** 075304
[8] Tran D V, Zheng H Y, Lam Y C, Murukeshan V M, Chai J C and Hardt D E 2005 *Opt. Laser Eng.* **43** 977
[9] Lorazo P, Lewis L J and Meunier M 2003 *Phys. Rev. Lett.* **91** 225502
[10] Chen M, Liu X D, Zhao M W, Chen C S and Man B Y 2009 *Phys. Rev. E* **80** 016405
[11] Chen M, Liu X D, Zhao M W and Sun Y M 2009 *Opt. Lett.* **34** 2682
[12] Chen M, Liu X D, Liu Y H and Zhao M W 2012 *J. Appl. Phys.* **111** 103108
[13] Chen M, Liu X D, Xia Y Y, Yang X M, Zhao M W, Sun Y M, Qi H J, Chen X F and Xu X G 2008 *Phys. Lett. A* **372** 5891
[14] Malkin A Y, Semakov A V and Kulichikhin V G 2010 *Adv. Coll. Interface Sci.* **157** 75
[15] Mckinley G H, Byars J A, Brown R A and Armstrong R C 1991 *J. Non-Newton. Fluid Mech.* **40** 201
[16] Werwa E, Seraphin A A, Chiu L A, Zhou C and Kolenbrander K D 1994 *Appl. Phys. Lett.* **64** 1821
[17] Craciun V, Bassim N, Singh R K, Craciun D, Hermann J and Boulmer-Leborgne C 2002 *Appl. Surf. Sci.* **186** 288
[18] Li Y and Qu S L 2012 *Chin. Phys. B* **21** 034208
[19] Yang Y N, Yang B, Zhu J R, Shen Z H, Lu J and Ni X W 2008 *Chin. Phys. B* **17** 1318
[20] Shieh J M, Chen Z H, Dai B T, Wang Y C, Zaitsev A and Pan C L 2004 *Appl. Phys. Lett.* **85** 1232
[21] Giacomo A D and Pascale O D 2004 *Thin Solid Films* **453–454** 328